Synthesis and structural identification of 3,6-Bis(3,5- dimethylpyrazol-1-yl)-1,2,4,5-tetrazine (BDT)

Hoang Trung Huu*, Nguyen Van Dung, Ha Dinh Viet

Le Quy Don Technical University, 236 Hoang Quoc Viet, Bac Tu Liem, Ha Noi, Vietnam.
*Corresponding author: hoanghuu@lqdtu.edu.vn
Received 07 Aug. 2024; Revised 17 Sep. 2024; Accepted 18 Sep. 2024; Published 14 Oct. 2024.
DOI: https://doi.org/10.54939/1859-1043.j.mst.IPE.2024.32-39

ABSTRACT

3,6-Bis(3,5-dimethylpyrazol-1-yl)-1,2,4,5-tetrazine (BDT) has emerged as a key intermediate for accessing other promising tetrazine-based high-energy-density compounds. The study presented the step-by-step process of synthesizing BDT while thoroughly analyzing and investigating its crystal structure. The chemical structure of BDT was characterized using spectroscopic techniques such as FT-IR, ^{1}H-NMR, ^{13}C-NMR, and data from PXRD and CCDC 254069. BDT was analyzed using various theoretical techniques, such as 2D fingerprint and Hirshfeld surface. The morphology of the BDT crystals was evaluated through optical microscope images. The results show that BDT crystallizes in a monoclinic space group P21/c, with four molecules per unit cell (Z=4) with the calculated lattice parameters as follows: a = 11.37 Å, b = 16.67 Å, c = 7.74 Å. The proportion of interactions of N...H and H...H of the total Hirshfeld surface area of BDT were 31.9% and 45.7%, respectively. ESP's maximum negative and positive values are -212.9 kJ.mol^{-1} and 65.6 kJ.mol^{-1}, respectively.

Keywords: BDT; Synthesis; Optimization structure; DFT.

1. INTRODUCTION

1,2,4,5-Tetrazine, also known as s-tetrazine, is a six-membered aromatic heterocyclic compound containing four nitrogen atoms. S-Tetrazine derivatives have attracted great interest in recent years as high-energy density materials (HEDMs) due to their unique combination of properties, including high enthalpy of formation, good thermal stability, low sensitivity to external stimuli, and high nitrogen content [1-3].

With nitrogen contents exceeding 60%, s-tetrazines significantly exceed the nitrogen levels in conventional energetic materials. This makes them promising candidates to replace traditional explosives, propellants, and gas generators, allowing higher energy density and more environmentally friendly decomposition products like N_2, HCN, and HN_3 [4]. Extensive work has been done to synthesize various s-tetrazine derivatives and characterize their properties [5-10]. Strategies to improve oxygen balance and density include introducing energetic functional groups like nitro, nitramine, azide, and guanidine.

Some key research on s-tetrazines has involved synthesizing derivatives through methods developed by Hiskey and Klapötke [11, 12]. Specific compounds like BDT, DAAT, BTATz, and DIAT have been made and characterized. Properties, including thermal stability, sensitivity, enthalpy of formation, oxygen balance, and combustion products, have been evaluated. S-tetrazines have been established as promising candidates for advanced high-energy density materials, but questions about their synthesis and applications remain.

3,6-Bis(3,5-dimethylpyrazol-1-yl)-1,2,4,5-tetrazine (BDT) has emerged as a key intermediate for accessing other promising tetrazine-based high-energy-density compounds. Simultaneously, they can act as ligands to synthesize important complexes. In recent years, BDT has been employed in some pyrotechnic compositions and the manufacture of spherical propellants [13]. In reference

[5], the elucidation of the structure and synthetic mechanism of 3,6-Bis(3,5-dimethylpyrazol-1-yl)-1,4-dihydro-1,2,4,5-tetrazine (HBDT) as an intermediate to produce BDT has been provided. BDT has been extensively synthesized as an intermediate in organic reactions. However, synthesizing BDT with high purity and suitable particle sizes remains a significant challenge, and there is currently no comprehensive publication regarding the structural and physicochemical properties, molecular bonding, and interactions of BDT.

In this article, we present the method of synthesis of BDT through intermediate products (HBDT), as well as the methods to identify them. The structure and purity of BDT were determined by FTIR infrared spectroscopy and nuclear magnetic resonance (NMR) spectroscopy. Moreover, BDT was analyzed using various theoretical techniques, such as 2D fingerprint and Hirshfeld surface.

2. MATERIALS AND METHODS

2.1. Materials

The chemicals used for synthesizing BDT include guanidine hydrochloride ($CH_5N_3.HCl$) with a purity of 97%; ethanol (C_2H_5OH) at a concentration of 99.7%; hydrazine hydrate ($N_2H_4.H_2O$) with an 80% concentration; 2,4-pentane-dione ($C_5H_8O_2$) at a concentration of 99%; acetic acid (CH_3COOH) with a concentration of 99.5%, and sodium nitrite ($NaNO_2$) with a purity of 99% was provided by Xilong Scientific Co., Ltd., China, and these solvents were of analytical grade.

2.2. Methods

2.2.1. Synthesis of BDT

General caution. The titled compounds are energetic and tend to combust or even explode under certain conditions. It is necessary to take appropriate safety precautions (safety glasses, face shields, and leather coats). The synthesis of BDT is a three-step process starting from guanidine hydrochloride [14]:

Add 35 g (0.366 mol) of guanidine hydrochloride to 220 ml of ethanol (90-96%) at room temperature. Add 88 ml (1.468 mol) of hydrazine hydrate (80%, ρ=1.04 g.cm^{-3}) and stir for 1.5 hours. Then, the solution is boiled and continued stirring for 10 hours. During the reaction, a white crystalline substance (TAG.HCl) is formed. When the reaction is complete, the solution is cooled to room temperature. The product is filtered and washed with ethanol, then dried in air, and 45.51 g of TAG.HCl is obtained, yielding 88.5%.

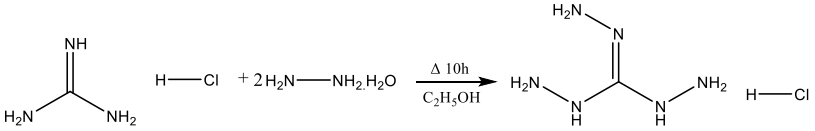

Scheme 1. *Synthesis of TAG.HCl.*

40 g (0.285 mol) of TAG.HCl was added to 250 ml of water at 0-5 °C, and 59 ml of 2,4-pentanedione was slowly added. As the addition occurred, the reaction solution became yellow-orange. The temperature was maintained for 30 minutes. Then, the solution was heated to 25 °C and held for 30 minutes. Subsequently, the reaction solution was heated to 70 °C and maintained at this temperature for 1.5 hours. A yellow-orange suspension formed over this period. When the reaction was complete, the solution was cooled to 15 °C. The product was filtered, washed with triple the volume of water (750 ml), and dried in a vacuum oven at 50 °C. 32.88 g of a pale yellow crystalline compound (HBDT) was obtained, yielding 84.4%.

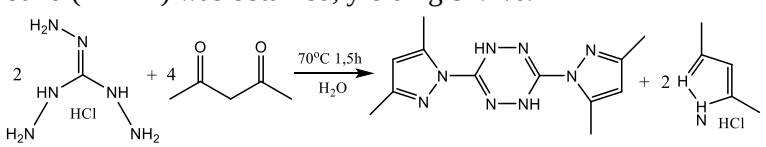

Scheme 2. *Synthesis of HBDT.*

With stirring, 15 g (0.055 mol) of HBDT was added to 210 ml of acetic acid (ρ = 1.05 g/cm^{-3}) at room temperature. 7.6 g (0.11 mol) of sodium nitrite was slowly added. During the addition, the reaction solution changed from pinkish red to purple red, with reddish brown gas evolving. After adding sodium nitrite was complete, the reaction solution was stirred for 2 hours. The resulting solution was then diluted with three times the volume of water (600 ml) at room temperature with stirring and allowed to settle for 15 minutes. The product was filtered, washed with water until neutralization, and dried in a vacuum oven at 60 °C. 12.89 g of brick red crystalline compound (BDT) was obtained, yielding 86.6%.

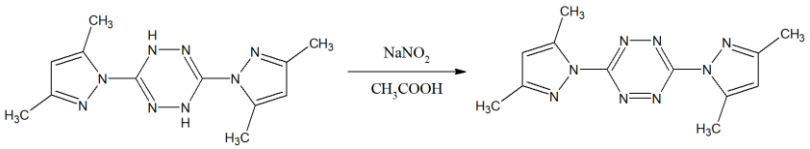

Scheme 3. *Synthesis of BDT.*

2.2.2. Experimental techniques

The ^{1}H and ^{13}C-NMR spectra were recorded using the Bruker Avance NMR spectrometer at a frequency of NEO 600 MHz, with the residual solvent peak as a reference. Chemical shifts are reported in ppm (δ). The IR spectra were also measured using the Perkin-Elmer Spectrum 400 spectrometer, with a range of 400-4000 cm^{-1} and a resolution of 2 cm^{-1}.

To ensure accuracy in X-ray determination, the BDT crystals obtained through crystallization undergo a four-hour vacuum drying process before use. The PXRD experiments were conducted through a Bruker D8 Advance apparatus, and the structures were solved via direct methods with X'Pert HighScore Plus software, utilizing crystallographic data from CCDC 254069. These data are free from The Cambridge Crystallographic Data Centre and are accessible via www.ccdc.cam.ac.uk.

2.2.3. Computational techniques

The crystal packing calculation required a geometric optimization of all structures. This was done using the DFT/B3LYP functional with a standard 6-31G* basis set. All the calculations were carried out using the Gaussian09 software package [15]. To obtain Hirshfeld surfaces and 2D fingerprint plots of the BDT, the Crystal Explorer software [16] was used.

3. RESULTS AND DISCUSSION

3.1. Structure determination

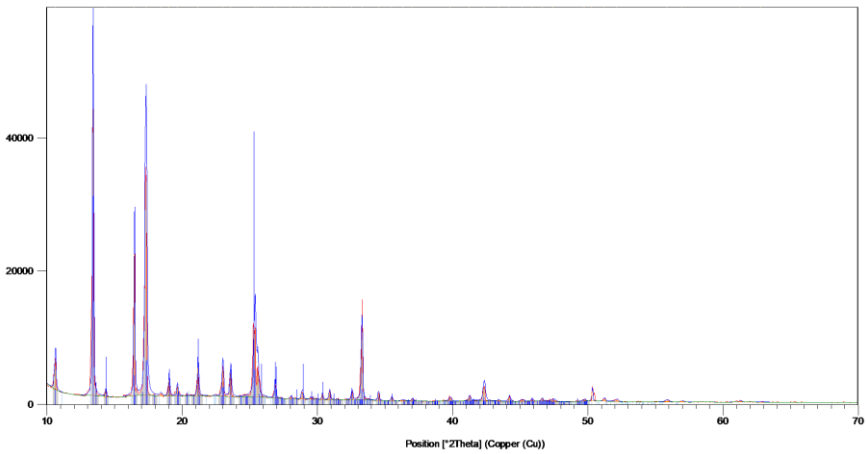

Fig. 1. *The PXRD patterns of BDT.*

The BDT crystals were purified using ethyl acetate and dried. The resulting crystals were analyzed through PXRD, and the structure of the synthesized BDT was determined using CCDC 254069 and lattice parameter calculations.

The PXRD data for the synthesized BDT in figure 1 closely matches the data from CCDC 254069. The lattice parameters for BDT are calculated to be a = 11.37 Å, b = 16.67 Å, c = 7.74 Å. In addition, figure 2 provides molecular structure views of BDT. BDT crystallizes in a monoclinic space group P21/c, with four molecules per unit cell (Z=4), and has a crystal density of 1.38 $g.cm^{-3}$ at room temperature. figure 2b showcases the 2D layered structure and mesh hydrogen-bond structure of the crystal, while figure 2c displays the intermolecular interactions of BDT. The selected bond distances and angles are listed in table 1.

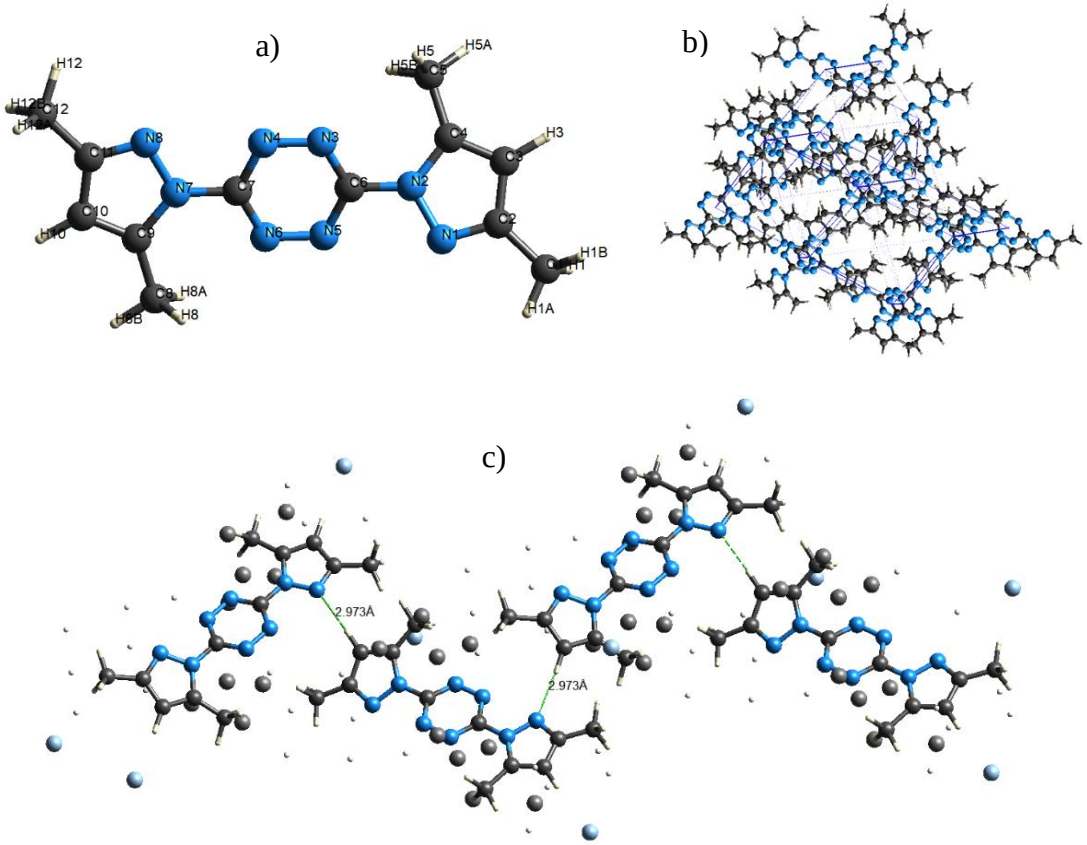

Fig. 2. *(a) Crystal structure of BDT, (b) Supramolecular structure of BDT, (c) Intermolecular interactions of BDT.*

Table 1. *Selected bond lengths (Å) and bond angles (°) of BDT.*

Bond	Dist.	Bond	Dist.	Bond	Dist.
N(1)–C(2)	1.333	N(4)–C(7)	1.358	N(7)–C(7)	1.382
N(1)–N(2)	1.432	N(5)–N(6)	1.354	N(8)–C(11)	1.333
N(2)–C(4)	1.404	N(5)–C(6)	1.358	C(4)–C(5)	1.499
N(2)–C(6)	1.382	N(6)–C(7)	1.355	C(3)–C(4)	1.373
N(3)–C(6)	1.355	N(7)–N(8)	1.432	C(2)–C(3)	1.432
N(3)–N(4)	1.354	N(7)–C(9)	1.404	C(1)–C(2)	1.499

Angle	(°)	Angle	(°)	Angle	(°)
C(6)–N(3)–N(4)	118.35	N(3)–C(6)–N(2)	116.81	N(7)–C(7)–N(6)	116.81
C(7)–N(4)–N(3)	116.18	C(6)–N(2)–C(4)	129.77	C(2)–C(3)–C(4)	107.31
C(6)–N(5)–N(6)	116.18	N(8)–C(11)–C(12)	120.51	C(1)–C(2)–C(3)	127.33
N(3)–C(6)–N(5)	125.44	C(10)–C(9)–C(8)	128.29	N(2)–C(4)–C(3)	105.43
C(7)–N(6)–N(5)	118.35	N(1)–C(2)–C(1)	120.51	C(7)–N(7)–N(8)	118.66

The intermediate product (HBDT) and the final product (BDT) are represented as light yellow and bright red compounds in figures 3a and 3b. The conclusive characterization of BDT was accomplished through a comprehensive analysis employing two standard techniques, namely Fourier-transform infrared spectroscopy (FTIR) and nuclear magnetic resonance (NMR).

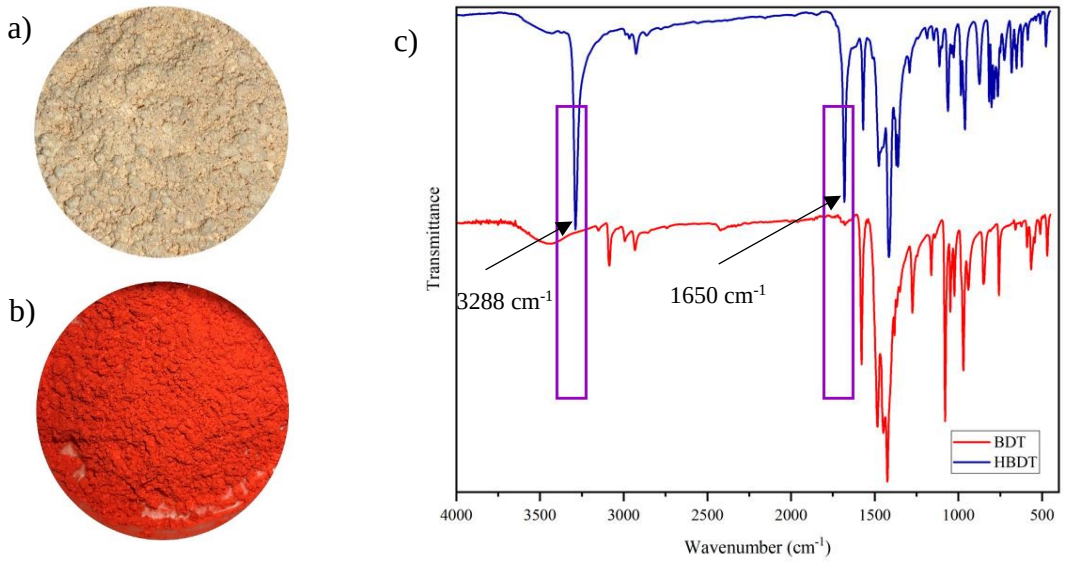

Fig. 3. *The images of HBDT (a), BDT (b), and the FTIR spectra of HBDT and BDT (c).*

Figure 3c displays the FTIR spectrum of BDT compared to the intermediate compound (HBDT). The functional groups present in the spectra are identified as follows: the peak at 3085 cm^{-1} indicates the characteristic stretching vibration of the (=C–H) bond; peaks at 2992 and 2852 cm^{-1} represent symmetric stretching vibrations of ($–CH_2$s); the peak at 2930 cm^{-1} denotes the asymmetric stretching vibration of ($–CH_3$as). The peaks observed at 1448, 1080, 970, and 565 cm^{-1} indicate vibrations characteristic of the tetrazine's ring, while the peak at 1483 cm^{-1} corresponds to the pyrazole's ring. Furthermore, the FTIR spectrum differentiates HBDT from BDT by highlighting the 3288 and 1650 cm^{-1} peaks within the HBDT spectrum, representing stretching and deformation vibrations of the –N–H bond within the tetrazine's ring.

The synthesized compound BDT underwent dissolution in Deuterated Chloroform ($CDCl_3$) and subsequent analysis through nuclear magnetic resonance (NMR) spectroscopy, specifically ^{1}H-NMR and ^{13}C-NMR, to elucidate its structural configuration. The ^{1}H-NMR spectrum, as depicted in Fig. 4a, displayed distinctive chemical shift values at δ=2.39 (s, 6H); 2.72 (s, 6H); 6.20 (s, 2H) ppm. Upon comparison with the known structure of BDT, these shifts were found to align precisely with the anticipated positions of hydrogen atoms, successively attributed to two methyl groups and a CH moiety situated on the pyrazole's ring. Figure 4b illustrates the ^{13}C-NMR spectrum, manifesting characteristic chemical shift values at δ=13.85 (C1, C12); 14.65 (C5, C8); 111.89 (C3, C10); 143.77 (C4, C9); 154.45 (C2, C11); 159.31 (C6, C7) ppm. These values correspond closely

to the anticipated positions of carbon atoms, sequentially ascribed to two methyl groups, three carbons on the pyrazole's ring, and a carbon atom on the tetrazine's ring, following the proposed structural model.

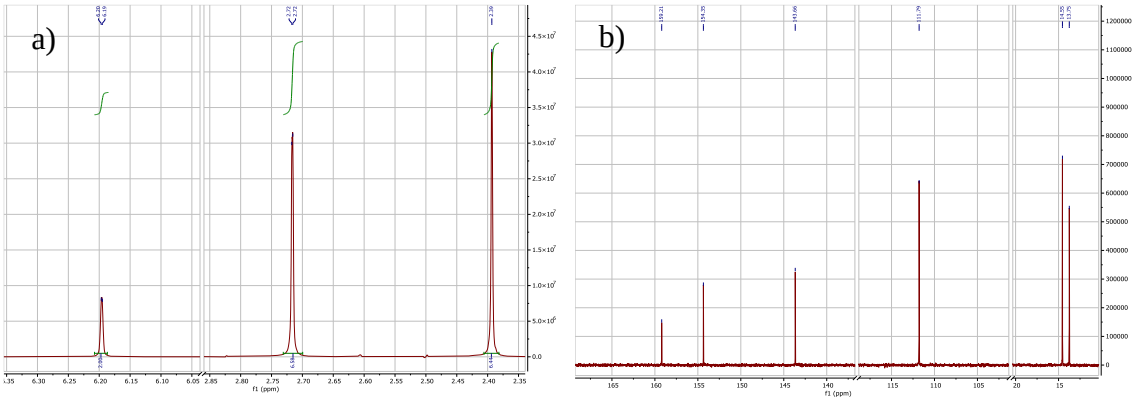

Fig. 4. *^{1}H-NMR (a) and ^{13}C-NMR (b) spectra of BDT.*

3.2. Intermolecular interaction and molecular electrostatic potentials analysis

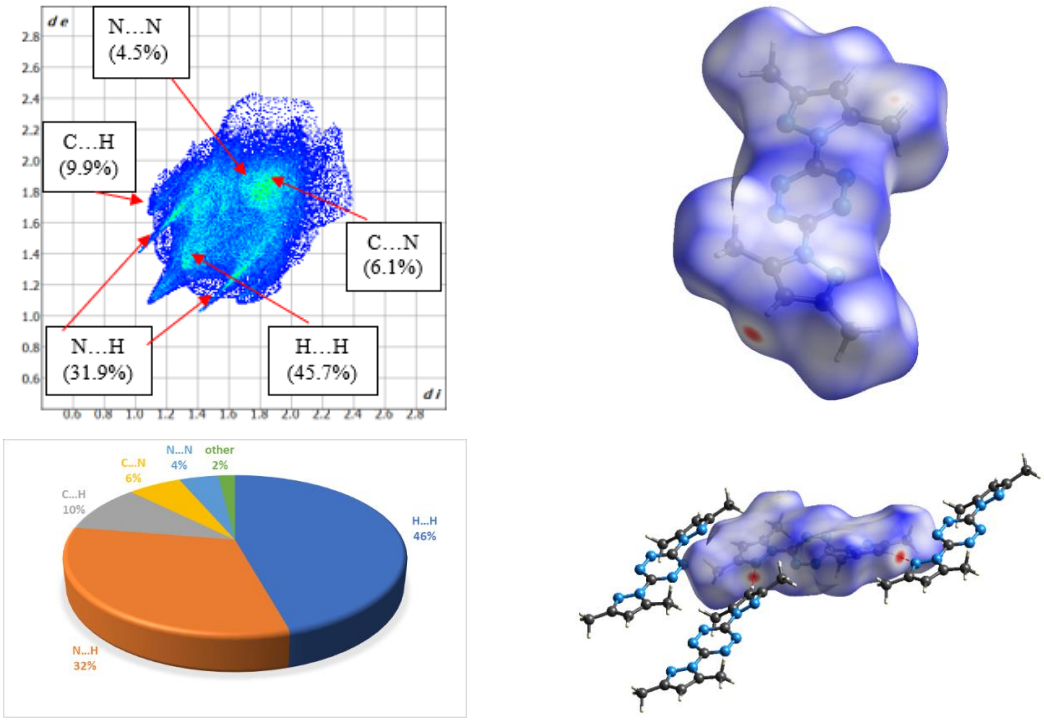

Fig. 5. *The Hirshfeld surface and 2D-Fingerprint plot for BDT.*

The different types of interactions between molecules can be analyzed through Hirshfeld surface analysis. Using Crystal Explorer, the Hirshfeld surface and 2D fingerprint plots of the experimental crystal structure of BDT were obtained. The Hirshfeld surface and 2D fingerprint plots of BDT are shown in figure 5. The red and blue areas on the Hirshfeld surface indicate increased and decreased proximity between molecules. Due to BDT's flat configuration, there are noticeable red zones around the edges of its surface, suggesting either weak interactions or strong hydrogen bonds within its crystal structure.

For each point on the Hirshfeld surface, the normalized contact distance (*norm*) is determined

by the below eq:

$$d_{norm} = \frac{(d_i - d_i^{vdW})}{r_i^{vdW}} + \frac{(d_e - d_e^{vdW})}{r_e^{vdW}} \quad (1)$$

d_i and d_e are measured from the surface to the nearest atom interior and from the nearest atom exterior to the surface interior, respectively, where r_i^{vdW} and r_e^{vdW} are the van der Waals radii of the atoms. In addition, the shorter $d_i + d_e$ of the spikes suggests stronger hydrogen bonds (N...H and H...N interactions). It can be seen from Fig. 5 that the proportion of interactions of N...H and H...H of the total Hirshfeld surface area of the BDT were 31.9% and 45.7%, respectively.

The electrostatic potential V(r) depicts the static charge distribution within a molecule. This property proves highly beneficial for analyzing and predicting molecular reaction behavior and pinpointing specific locations or regions within a molecule that initially attract approaching electrophiles/nucleophiles. The calculated electrostatic potentials (ESP) of BDT are shown in Fig. 6.

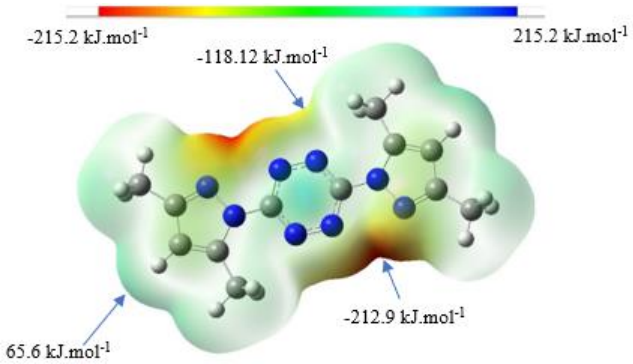

Fig. 6. *Molecular electrostatic potentials of BDT calculated with B3LYP/6-31G* basis set.*

The MEP was calculated at a B3LYP/6-31G* optimized geometry to predict reactive sites for electrophilic and nucleophilic attack for the BDT studied. MEP's positive regions (blue) are related to nucleophilic reactivity, and the negative areas (red) are related to electrophilic reactivity. The maximum positive value of ESP is -212.9 kJ.mol^{-1} and is located between the N(1, 8) nitrogen atom of the pyrazole ring and the tetrazine motif. On the contrary, the maximum negative value of ESP is 65.6 kJ.mol^{-1} and is located at the CH fragment of the pyrazole ring.

This explains why BDT is a compound susceptible to attack by nucleophiles at the N(2) and N(7) positions on the pyrazole ring, especially with O, N, and S-nucleophiles.

4. CONCLUSIONS

In summary, 1,2,4,5 tetrazine derivative, namely, 3,6-Bis(3,5-dimethylpyrazol-1-yl)-1,2,4,5-tetrazine (BDT), has been synthesized and characterized by FTIR, 1H-NMR, 13C-NMR. The lattice parameters were calculated using data from the PXRD experiment and CCDC 254069. The result shows that BDT crystallizes in a monoclinic space group P21/c, with four molecules per unit cell (Z=4) with the calculated lattice parameters as follows: a = 11.37 Å, b = 16.67 Å, c = 7.74 Å. The Hirshfeld surface, 2D-Fingerprint plot, and ESP of BDT were calculated and analyzed. The proportion of interactions of N...H and H...H of the total Hirshfeld surface area of the BDT were 31.9% and 45.7%, respectively. ESP's maximum negative and positive values are -212.9 kJ.mol^{-1} and 65.6 kJ.mol^{-1}, respectively.

REFERENCES

[1]. Sifain, A.E., et al., "*Photoactive excited states in explosive Fe (II) tetrazine complexes: A time-dependent density functional theory study*". J. Phys. Chem. C. **Vol. 120,** No. 50, pp. 28762-28773, (2016).

[2]. Chavez, D.E., M.A. Hiskey, and R.D. Gilardi, "*3, 3'-Azobis (6-amino-1, 2, 4, 5-tetrazine): A Novel High-Nitrogen Energetic Material".* Angew. Chem., Int. Ed. Engl. **Vol. 39,** No. 10, pp. 1791-1793, (2000).
[3]. Coburn, M., et al., "*Oxidations of 3, 6-diamino-1, 2, 4, 5-tetrazine and 3, 6-bis (s, s-dimethylsulfilimino)-1, 2, 4, 5-tetrazine".* J. Heterocycl. Chem. **Vol. 30,** No. 6, pp. 1593-1595, (1993).
[4]. Sinditskii, V., et al., "*Thermal behavior and combustion mechanism of high-nitrogen energetic materials DHT and BTATz".* Thermochim. Acta. **Vol. 535**, pp. 48-57, (2012).
[5]. Zhang, J.G., et al., "*The Crystal Structure and Synthesis Mechanism of 3, 6-Bis (3, 5-dimethylpyrazol-1-yl)-1, 4-dihydro-1, 2, 4, 5-tetrazine (BDT): A Key Precursor of S-tetrazine".* J. Heterocycl. Chem. **Vol. 51,** No. S1, pp. E234-E240, (2014).
[6]. Zhang, T., et al., "*Alkali metal salts of 3, 6-dinitramino-1, 2, 4, 5-tetrazine: Promising nitrogen-rich energetic materials".* CrystEngComm. **Vol. 21,** No. 4, pp. 765-772, (2019).
[7]. Stetsiuk, O., A. Abhervé, and N. Avarvari, "*1, 2, 4, 5-Tetrazine based ligands and complexes".* Dalton Trans. **Vol. 49,** No. 18, pp. 5759-5777, (2020).
[8]. Ren, J., et al., "*3-Nitramino-6-hydroxy-1, 2, 4, 5-tetrazine and its alkaline earth metal salts: an effective strategy to balance energy density and safety of energetic compounds".* J. Energ. Mater. **Vol. 39,** No. 1, pp. 48-59, (2021).
[9]. Li, H., et al., "*Nitrogen-rich salts of 3, 6-dinitramino-1, 2, 4, 5-tetrazine: syntheses, structures, and energetic properties".* J. Energ. Mater. **Vol. 40,** No. 1, pp. 15-33, (2022).
[10]. Hu, L., et al., "*Selecting suitable substituents for energetic materials based on a fused triazolo-[1, 2, 4, 5] tetrazine ring".* ACS Appl. Energy Mater. **Vol. 3,** No. 6, pp. 5510-5516, (2020).
[11]. Klapoetke, T.M., et al., "*Highly Energetic Salts of 3, 6-Bishydrazino-1, 2, 4, 5-tetrazine".* Cent. Eur. J. Energetic Mater. **Vol. 10,** No. 2, pp. 151-170, (2013).
[12]. Klapoetke, T.M., A. Preimesser, and J. Stierstorfer, "*Thermally Stable 3, 6-Disubstituted 1, 2, 4, 5-Tetrazines".* Z. fur Naturforsch. - B J. Chem. Sci. **Vol. 68,** No. 12, pp. 1310-1320, (2013).
[13]. Steinhauser, G. and T.M. Klapötke, "*"Green" pyrotechnics: a chemists' challenge".* Angew. Chem., Int. Ed. Engl. **Vol. 47,** No. 18, pp. 3330-3347, (2008).
[14]. Gong, Y.-H., "*Synthesis electrochemical and fluorescence studies of 1, 2, 4, 5-tetrazine derivatives: towards molecular sensors for anions and electron-rich compounds and synthesis and electrochemical study of ferrocene-containing pyridinium salts"*, Cachan, Ecole normale supérieure, (2007).
[15]. Frisch M. J., e.a., "*Gaussian 09, revision A. 01. Gaussian"*, Inc.: Wallingford, CT, (2009).
[16]. Spackman, P.R., et al., "*CrystalExplorer: A program for Hirshfeld surface analysis, visualization and quantitative analysis of molecular crystals".* J. Appl. Crystallogr. **Vol. 54,** No. 3, pp. 1006-1011, (2021).

TÓM TẮT

Tổng hợp và định danh cấu trúc hợp chất 3,6-Bis(3,5- dimethylpyrazol-1-yl)-1,2,4,5-tetrazine (BDT)

3,6-Bis(3,5-dimethylpyrazol-1-yl)-1,2,4,5-tetrazine (BDT) là một hợp chất trung gian đầy hứa hẹn để tổng hợp các hợp chất mật độ dị vòng năng lượng cao khác dựa trên cơ sở vòng tetrazine. Bài báo trình bày quy trình từng bước tổng hợp BDT, phân tích và nghiên cứu cấu trúc tinh thể của nó. Cấu trúc hóa học của BDT được xác định bằng các phương pháp như FT-IR, ^{1}H-NMR, ^{13}C-NMR và dữ liệu từ PXRD và CCDC 254069. BDT được phân tích bằng nhiều kỹ thuật lý thuyết khác nhau như 2D fingerprint và diện tích bề mặt Hirshfeld. Hình ảnh tinh thể của BDT được xác định bằng hình ảnh trên kính hiển vi quang học. Kết quả đo đạc và tính toán cho thấy, BDT kết tinh ở dạng đơn tà nhóm P21/c, với bốn phân tử trên một ô đơn vị (Z = 4) với các tham số mạng tinh thể được tính toán như sau: a = 11,37 Å, b = 16,67 Å, c = 7,74 Å. Tỷ lệ tương tác của N...H và H...H trên tổng diện tích bề mặt Hirshfeld của BDT lần lượt là 31,9% và 45,7%. Giá trị thế tĩnh điện âm và dương tối đa của BDT lần lượt là -212,9 kJ.mol^{-1} và 65,6 kJ.mol^{-1}.

Từ khóa: BDT; Tổng hợp; Tối ưu hóa cấu trúc; DFT.